ISBN: 978-3-95450-262-2 ISSN: 2673-5350 doi: 10.18429/JACoW-IBIC2025-WEBI01

SIMULTANEOUS MEASUREMENTS WITH FAST BEAM SIZE AND POSITION MONITORS DISENTANGLE THE SUDDEN BEAM LOSS EVOLUTION MECHANISM

G. Mitsuka*,[1], KEK, Tsukuba, Ibaraki, Japan
R. Nomaru, University of Tokyo, Bunkyo, Japan
T. Ishida, S. Iwabuchi, H. Ikeda[1], T. Mitsuhashi[1], KEK, Tsukuba, Ibaraki, Japan
[1]also at Sokendai, the Graduate University for Advanced Studies, Hayama, Kanagawa, Japan

Content from this work may be used under the terms of the CC BY 4.0 licence (© 2024). Any distribution of this work must maintain attribution to the author(s), title of the work, publisher, and DOI.

Abstract

At the SuperKEKB electron-positron collider, which aims to achieve the world's highest luminosity, "Sudden Beam Loss (SBL) events" have prevented its stable operation, in which several tens of percent of the beam current is lost and aborted within several turns (20 µs–50 µs). Elucidating SBLs, which can cause extensive damage to accelerator components and the Belle II experiment detectors, is a pressing issue for SuperKEKB. To measure the beam size and position variation, key information for disentangling SBLs, over dozens of turns just before the SBL-induced beam aborts, we have developed new turn-by-turn beam size monitors in two different wavelength regions, X-ray and visible light, and bunch-by-bunch beam position monitors where one has utilized a novel architecture AMD/Xilinx RFSoC. Simultaneous measurements of turn-by-turn beam size and bunch-by-bunch beam position enable elucidation of the cause and time evolution mechanism of the SBL events. We will introduce recently developed fast beam size and beam position monitors, then show their simultaneous measurements of SBL events. We will also discuss the possible causes and time evolution mechanisms of the SBL events.

INTRODUCTION

The SuperKEKB accelerator is a collider consisting of a 7 GeV electron ring (the high-energy ring, HER) and a 4 GeV positron ring (the low energy ring, LER). As indicated in Fig. 1, the highest luminosity recorded by SuperKEKB in 2024 December was 5.1×10^{34} cm^{-2} s^{-1}, which is the world record as of 2025 August. On the other hand, to achieve SuperKEKB's target 6×10^{35} cm^{-2} s^{-1}, it is clear that further beam current enhancement and beam operation stabilization are needed.

The biggest obstacle to the current enhancement and long-term stability of beam operation is Sudden Beam Loss (SBL) events [1,2]. SBL events occur when the beam (bunch) orbit suddenly begins to oscillate without any obvious precursor, and more than 10 % of the beam current is lost in just a few turns (tens of microseconds), leading to beam abort. Figure 2 indicates an example of a SBL event in LER. The top two panels show the bunch positions measured by Bunch Oscillation Recorders (BORs, monitors that can record the orbit of each bunch for more than 100 turns). The topmost panel shows the horizontal orbit, and the second panel shows

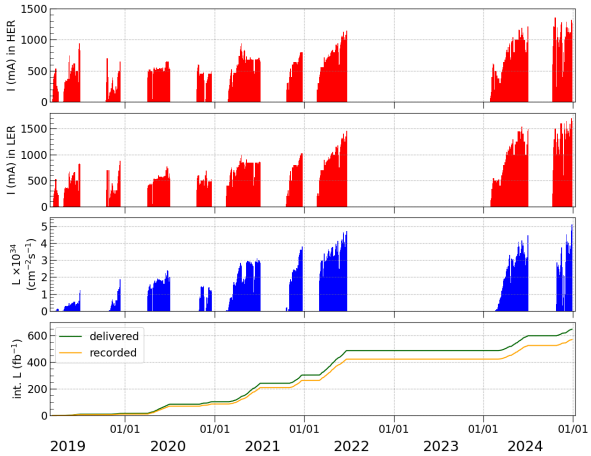

Figure 1: Luminosity record of the SuperKEKB collider in 2019–2024.

the vertical orbit. The horizontal axis represents the bunch train, and the vertical grid indicates divisions per turn. The leftmost division corresponds to 6 turns before beam abort. The third row shows the bunch current, normalized to 1 at the left edge of the plot. A beam loss occurred two turns before the abort, causing the current to drop. The bottom row expresses the beam loss in current (mA), showing a large loss immediately before the abort.

The SBL events can cause significant damage to the Belle II detectors and accelerator components in proportion to the beam current, so it is an urgent issue to elucidate the mechanism of the occurrence of such events and to take measures to suppress them. Analysis of data acquired by loss monitors and BORs installed at various locations in the ring [3] indicates that the occurrence of sudden beam loss events is caused by a change in bunch position or an increase in bunch size due to some reason, which leads to a collision with the collimator system. There are three possible patterns of bunch position and size changes, as shown in Fig. 3. *Pattern A* is a usual bunch, *Pattern B* is a bunch position variation, *Pattern C* is an increase in size, and *Pattern D* is a variation in position and size.

As discussed in Ref. [4], we developed a high-speed profile monitor that measures the beam size at each turn. In this study, by comparing the beam size measurement results with the bunch position measured by BOR and the bunch

* gaku.mitsuka@kek.jp

ISBN: 978-3-95450-262-2 ISSN: 2673-5350 doi: 10.18429/JACoW-IBIC2025-WEBI01

current and its loss measured by a bunch current monitor, we aim to discriminate the three patterns *B–D*, in which the bunch collides with the collimator and beam loss occurs, and elucidates the mechanism.

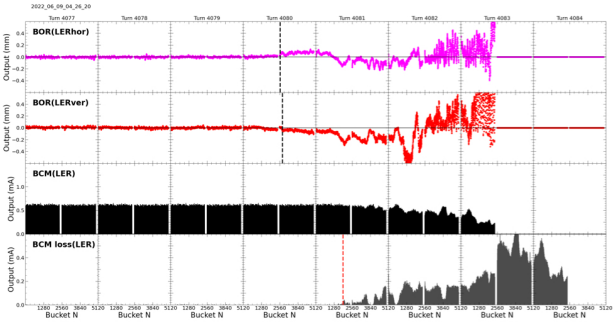

Figure 2: Example of a SBL event, where the horizontal orbit, vertical orbit, bunch charge, and bunch charge loss (multiplied by 5) are shown from the top.

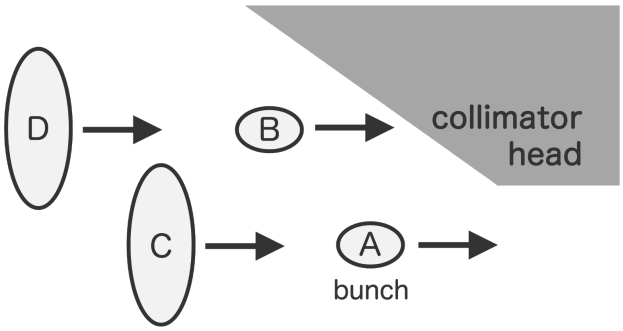

Figure 3: Patterns of SBL events.

X-RAY BEAM SIZE MONITOR

The X-ray beam size monitor [5] is the standard transverse beam size monitor in SuperKEKB. First, synchrotron radiation reaches an optical mask called a coded aperture located about 10 m downstream from the synchrotron radiation emission point. A coded aperture is randomly arranged multi-slits of different widths. Only X-rays that pass through the coded aperture reach the scintillator screen, which is located about 30 m further downstream. A CMOS camera measures the X-ray profile projected onto the screen, and the beam size is estimated by matching the measured profile with a simulated profile corresponding to a specific assumed beam size. For details on the imaging system based on a high-speed CMOS camera MIKROTRON EoSens 1.1CX12, refer to Ref. [4].

Figure 4 shows an example of an abort event in LER with beam size increase. This event was not qualified as a sudden beam loss event because no significant loss occurred. The horizontal axis in the top panel shows the number of turns, with the left edge of the plot set to 0 for convenience. Counting from the left edge of the plot, beam abort occurs at the 24th turn. In the top panel, the beam size (blue curve) 85 µm started to increase about 12 turns before the abort, reaching a maximum value of about 400 µm. Simultaneously with the abort, the light intensity (green curve) drops to the pedestal level. LERUV (Upward Vertical, middle panel) and LERDV (Downward Vertical, bottom panel) are the names of the vertical BORs installed in LER, and the betatron oscillation phases are separated by 90° apart from each other. The LERDV shows that the bunch position started oscillating slightly about 12 turns before the abort. The future task is to analyze the LERU(D)V and X-ray beam size monitor data in detail to separate positional oscillation from beam size increase.

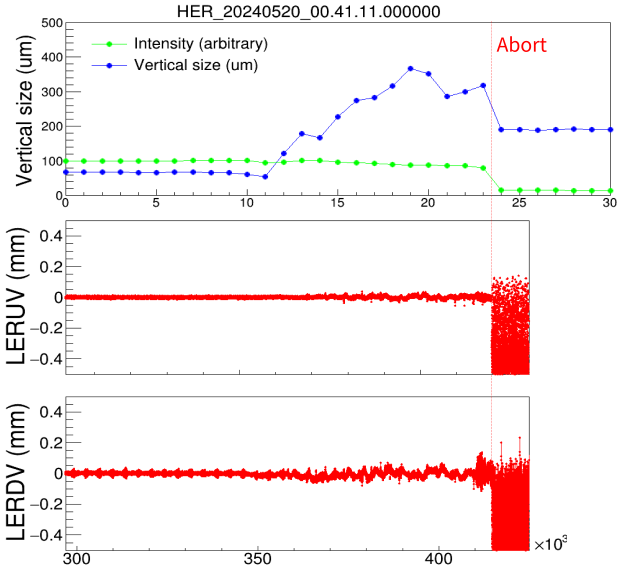

Figure 4: X-ray measurements for beam abort events in turn-by-turn vertical beam size (top) and bunch-by-bunch orbits (middle and bottom). The vertical bar indicates the timing of the beam abort.

VISIBLE-LIGHT BEAM SIZE MONITOR

The X-ray beam size monitors described in the previous section are suitable for beam size diagnostics with extremely short exposure times of only a few µs because of the high light intensity expected. X-ray beam size monitors must place their imaging systems in the SuperKEKB tunnel. As a result, they are susceptible to radiation from the electron and positron beams. Especially, the LER side of the X-ray beam size monitor is surrounded by the high-radiation HER injection section and dump system, which caused malfunctions of the CMOS camera and frame grabber.

Therefore, in addition to the high-speed X-ray beam size monitor, we developed a high-speed visible light beam size monitor. The visible light beamline is the same as the existing line installed during construction of SuperKEKB, and only the following profile detector system was newly developed. The optical system shown in Fig. 5 is based on the

Content from this work may be used under the terms of the CC BY 4.0 licence (© 2024). Any distribution of this work must maintain attribution to the author(s), title of the work, publisher, and DOI.

ISBN: 978-3-95450-262-2 ISSN: 2673-5350 doi: 10.18429/JACoW-IBIC2025-WEBI01

© Content from this work may be used under the terms of the CC BY 4.0 licence (© 2024). Any distribution of this work must maintain attribution to the author(s), title of the work, publisher, and DOI.

Gregorian telescope, which is the first stage of the coronagraph system [6] developed for beam halo measurements.

As detailed in Ref. [7], to extract synchrotron radiation from the vacuum chamber and guide it through a grass window into the atmospheric side, we installed a polycrystalline diamond extraction mirror in the vacuum chamber. The size of the extraction mirror 20 mm (W) × 31 mm (H) × 1.2 mm (D), positioned 23.6 m downstream from the synchrotron radiation source, determines the aperture. Figure 6 shows the simulated diffraction point spread function (PSF) results obtained using the optical design software Synopsys CODE V [8]. In the simulation, the PSF peak width is 120 µm, and the width must be corrected for the measured beam size.

Figure 7 shows an image of the synchrotron radiation made by the stored beam taken with the Gregorian telescope. Here the telescope's focus is put on the synchrotron radiation source. We see a well-focused beam core in the left panel and more than 15th-order diffraction fringes in the right panel.

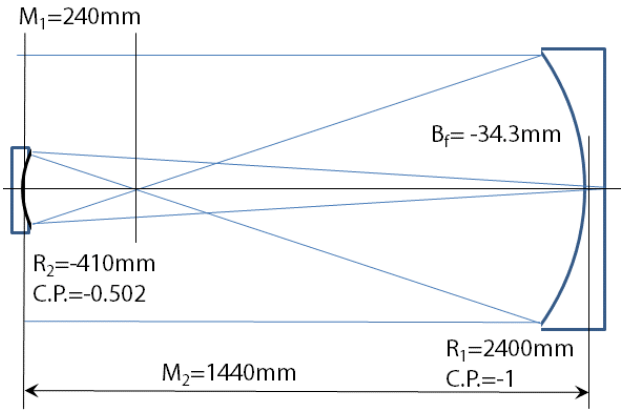

Figure 5: Schematic diagram of the Gregorian telescope.

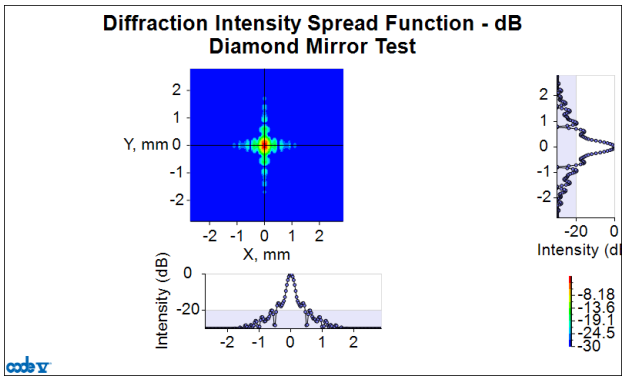

Figure 6: The simulated diffraction PSF results obtained using the Synopsys CODE V.

Figure 8 shows an SBL event in LER with beam size increase, occurring during a regular physics run. The top panel shows the beam size in pixels measured with the visible beam size monitor, and the bottom panel shows the bunch positions measured with the LERDV BOR. The timing of the beam size increase and the timing at which the bunch position measured by LERDV starts to oscillate are generally coincident.

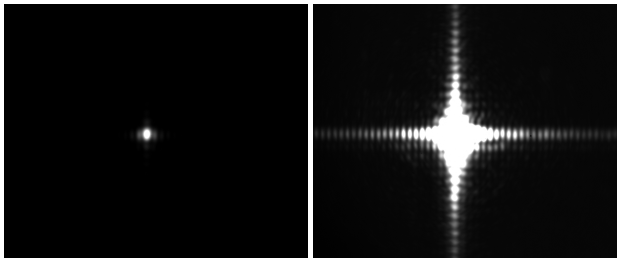

Figure 7: Diffraction pattern measurements for synchrotron radiation made with the Gregorian telescope. Left: Linear scale. Right: Logarithmic scale.

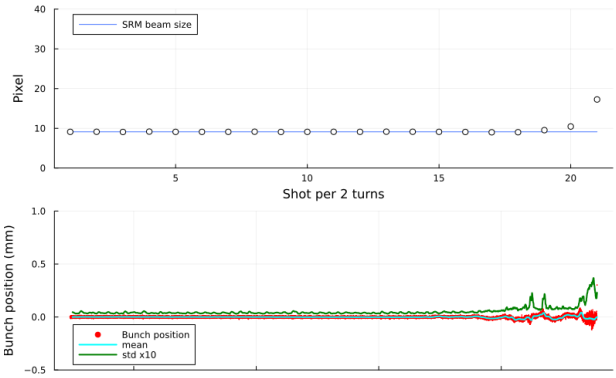

Figure 8: Visible-light measurements for SBL event in LER in vertical beam size in units of the CMOS sensor pixel (top) and bunch-by-bunch orbits measured with the LERDV BOR (bottom). The black markers in the top panel indicate shots every two turns. The SBL event occured on 29 Oct. 2024.

Here, attention should be paid to the correspondence between the pixel unit and the actual beam size in meters. To derive the coefficients of pixel / mm in this study, we first 1) move the position of the plane mirror on the horizontal stage placed just before the Gregorian telescope by 1 mm, 2) each time the distance moved by the center of the light image was measured in pixel units by a CMOS camera, 3) this operation was repeated dozens of times as long as the light image was within the CMOS sensor, 4) the data was linearly fitted to obtain the slope of the pixel distance relative to the mm distance. As seen in Fig. 9, the bestfit value of 32.35 pixel/mm was obtained. Dividing the Gregorian telescope's transverse magnification factor of 0.4 simulated by the Synopsys CODE V software by the design pixel size of the CMOS camera MIKROTRON EoSens 1.1CX12 13.7 µm/ pixel yields the estimated pixel / mm coefficient 29.20 pixel/mm. The measured pixel / mm coefficient results in <10 % different from the estimated coefficient.

Having obtained the peak width of the diffraction PSF and the pixel/mm conversion factor, we can derive the beam

ISBN: 978-3-95450-262-2 ISSN: 2673-5350 doi: 10.18429/JACoW-IBIC2025-WEBI01

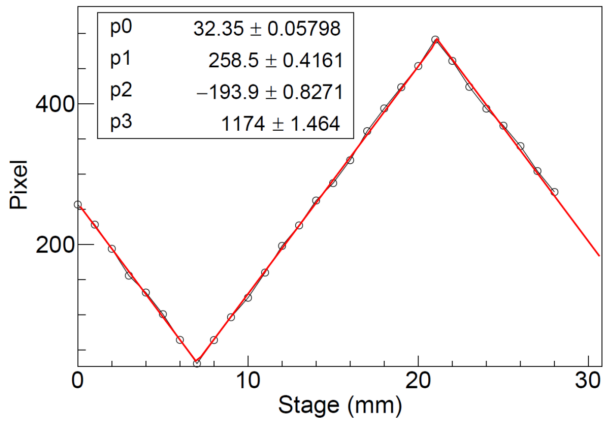

Figure 9: Metric units and pixel correspondence calibrated using the manual horizontal stage. Red lines indicate the bestfit results.

size in mm from the CMOS camera measurements. For verification, we will derive the beam size using two different methods under stable beam conditions and compare the results. Method 1 converts the visible light monitor measurement in units of pixel to mm units using the pixel / mm conversion coefficients, then subtracts the peak width of the diffraction PSF to determine the beam size. Method 2 predicts the beam size in mm using the beam size (mm) directly obtained from the X-ray monitor and the ratio of the vertical beta functions. Since the X-ray monitor has a measurement accuracy of 1 µm and the vertical beta function has a measurement accuracy within 5 %, the beam size from Method 2 can be used as a benchmark. Comparing Methods 1 and 2, assuming the measured values are correct, the peak width of the diffraction PSF should be approximately twice the simulation prediction, 250 µm. The discrepancy between the peak width predicted by simulation and that predicted from the comparison of Methods 1 and 2 remains unresolved. Possible causes include differences in the assumed wavelength distribution for the diffraction PSF calculation, optical system errors, and fitting errors in the lateral distribution of the observed synchrotron radiation. For simplicity in this analysis, the PSF peak width obtained from the comparison of Method 1 and Method 2 was used to derive the beam size in mm for a visible-light monitor.

Figure 10 shows the time-series variation of the beam size (top) and bunch position (bottom) for the same SBL event as in Fig. 8. The beam size was converted to mm using the method described above. The bunch position shown in the bottom panel indicates the measurements with the LERUV BOR for a better comparison with the bottom panel in Fig. 8. Five shots before the abort, i.e., 10 turns prior, the beam size was approximately 80 µm. This value naturally matches the beam size measurement from the X-ray monitor multiplied by the vertical beta function ratio. The beam size reached 450 µm immediately before the abort, indicating that the beam size increased by more than five times during the SBL event. This qualitatively agrees with the beam size increase measured by the X-ray monitor (see Fig. 4).

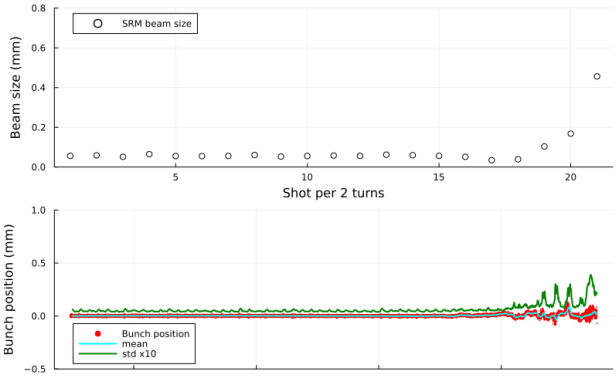

Figure 10: Visible-light measurements for SBL event in LER in vertical beam size in units of the CMOS sensor pixel (top) and bunch-by-bunch orbits measured with the LERUV BOR (bottom). The black markers in the top panel indicate shots every two turns. The SBL event occured on 29 Oct. 2024.

Next, we analyze the relationship between the increased beam size and the variation in bunch position. If the variation in bunch position is larger than the variation in bunch size, the measured beam size can be effectively considered a variation in bunch position. Conversely, if the variation in bunch position is sufficiently small compared to the measured beam size, the beam size can be considered an increase in bunch size. Figure 11 shows the maximum beam size and the maximum standard deviation of the bunch position. The standard deviation was derived from the bunch positions of a total of 450 bunches (equivalent to the number of bunches within the 2 µs exposure time frame of the visible light monitor). Given that the vertical beta function at the BOR measurement point is 19 m and the vertical beta function at the synchrotron radiation emission point is 67 m, a standard deviation of 0.10 mm corresponds to an visible beam size of 0.19 mm. Figure 11 shows that the visible beam size is significantly larger than the value estimated from the standard deviation of the bunch position variation, suggesting an increase in the bunch size.

Regardless of whether the variation of visible beam size is owing to bunch position or bunch size, an increase in visible beam size should result in beam loss. Figure 12 shows a comparison of beam size and beam loss. Beam loss is defined as the loss in the sum of bunch currents during the turn immediately preceding the abort, compared to the sum of bunch currents at least 20 turns prior to the abort. Although the statistics are limited, it appears that beam size also increases with beam loss. In events where losses exceeding 5 % were observed, the beam size increased by a factor of 3 to 5 times compared to the normal beam size of ~ 60 µs–80 µs.

Figure 13 shows beam loss with and without beam size increase. In 77 % of events where no beam size increase was observed, beam loss was within 1 %. Conversely, in events

Content from this work may be used under the terms of the CC BY 4.0 licence (© 2024). Any distribution of this work must maintain attribution to the author(s), title of the work, publisher, and DOI.

ISBN: 978-3-95450-262-2 ISSN: 2673-5350 doi: 10.18429/JACoW-IBIC2025-WEBI01

© Content from this work may be used under the terms of the CC BY 4.0 licence (© 2024). Any distribution of this work must maintain attribution to the author(s), title of the work, publisher, and DOI.

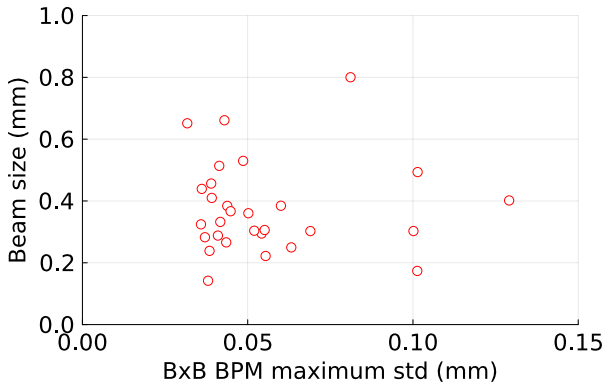

Figure 11: Maximum beam size and maximum standard deviation of the bunch position variation.

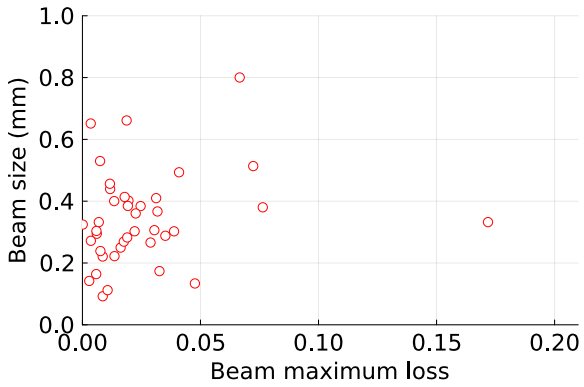

Figure 12: Maximum beam size and maximum beam loss.

where a beam size increase was observed, 68 % of the total exhibited beam loss of 1 % or more.

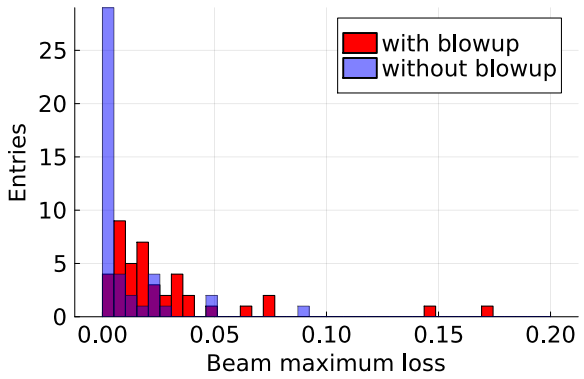

Figure 13: Fraction of beam loss events with and without beam size increase.

Here, we review the results of this analysis by applying them to the SBL occurrence patterns. In *Pattern B*, beam loss occurs when bunches collide with the collimator head due solely to positional fluctuations, without an increase in bunch size. This pattern should be distributed in the lower right region of Fig. 11; however, events with a standard deviation of bunch position fluctuations exceeding 0.15 mm did not exist in the population where beam size measurements were also performed simultaneously. Conversely, events where the positions of bunches within a bunch train coherently shift more than 1 mm in one direction can cause beam loss even with a small standard deviation. *Pattern C* involves events where the bunch size primarily increases, while the variation in bunch position is small. These events should be distributed in the upper left region of Fig. 11. In this study, many events were observed where the standard deviation of bunch position variation was around 0.05 mm, but the beam size increased to 0.3 mm–0.7 mm. This suggests an increase in bunch size and corresponds to *Pattern C*. *Pattern D*, where both bunch position and bunch size increase, should be distributed in the upper right of Fig. 11, but no such events were observed in this study.

Finally, we qualitatively compare collimator aperture and beam size increase. The head of the collimator with the narrowest aperture in LER (known as D06V1) is positioned 2.1 mm from the closed orbit. If part of the bunch collides with the collimator head, it leads to beam loss. As shown in Fig. 12, most beam loss is within 5 %. To cause a 5 % loss, the beam must reach twice the enlarged size (2σ), which is equivalent to 2.1 mm. However, in Fig. 12, the size of the population causing losses within 5 % is approximately < 0.7 mm, not reaching $2.1\,\mathrm{mm}/2 \sim 1$ mm. It should be noted here that the beam size monitor developed in this study measures the average beam size value of approximately 500 bunches, given an exposure time of 2 µs. On the other hand, if the bunch size has a considerable bunch-by-bunch variation, there is a possibility that bunches with large sizes will come into contact with the collimator.

In this study, we focused on the beam orbit variation and size increase to investigate why the beam loss of several tens of percent occurs for SBL events, however, the mechanism has not been clarified. To explore this possibility, we are developing an X-ray beam-size monitor that combines a silicon-strip sensor with an ADC capable of 2.7 GSPS. A new X-ray beam-size monitor enables bunch-by-bunch size measurements.

REFERENCES

[1] H. Ikeda *et al.*, "Observation of sudden beam loss in SuperKEKB", in *Proc. IPAC'23*, Venice, Italy, May 2023, pp. 716–719. doi:10.18429/JACoW-IPAC2023-MOPL072

[2] R. Nomaru, G. Mitsuka, L. Ruckman, "Measurement of Sudden Beam Loss Events Using Bunch-by-Bunch BPMs at SuperKEKB", arXiv:2507.13617v1. doi:10.48550/arXiv.2507.13617

[3] R. Nomaru, G. Mitsuka, L. Ruckman, and R. Herbst, "Development of a novel bunch oscillation recorder with RFSoC technology", *J. Instrum.*, vol. 19, p. P12026, 2024. doi:10.1088/1748-0221/19/12/P12026

[4] G. Mitsuka, T. Ishida, S. Iwabuchi, and R. Nomaru, "Measurements for beam size blowup in sudden beam loss events and analysis of the beam loss evolution mechanism", presented

ISBN: 978-3-95450-262-2 ISSN: 2673-5350 doi: 10.18429/JACoW-IBIC2025-WEBI01

at the IPAC'25, Taipei, Taiwan, Jun. 2025, paper THPS089, unpublished.

[5] E. Mulyani *et al.*, "First measurements of the vertical beam size with an X-ray beam size monitor in SuperKEKB rings", *Nucl. Instrum. Methods Phys. Res. A*, vol. 919, pp. 1–15, 2019. doi:10.1016/j.nima.2018.11.116

[6] G. Mitsuka, H. Ikeda, and T. M. Mitsuhashi, "Design and Construction of Optical System of the Coronagraph for Beam Halo Observation in the SuperKEKB", in *Proc. IPAC'22*, Bangkok, Thailand, Jun. 2022, pp. 769–771. doi:10.18429/JACoW-IPAC2022-TUOXGD1

[7] G. Mitsuka, H. Ikeda, and T. M. Mitsuhashi, "Renovation of the SR Beam Profile Monitors with Novel Polycrystalline Diamond Mirrors at the SuperKEKB Accelerator", in *Proc. IPAC'22*, Bangkok, Thailand, Jun. 2022, pp. 313–315. doi:10.18429/JACoW-IPAC2022-MOPOPT031

[8] D. C. O'Shea, J. L. Bentley, "Designing optics using CODE V", Bellingham, Washington USA, SPIE Digital Library, 2018. doi:10.1117/3.2319322

Content from this work may be used under the terms of the CC BY 4.0 licence (© 2024). Any distribution of this work must maintain attribution to the author(s), title of the work, publisher, and DOI.